Multiple-plateau structure and scaling relation in photoelectron spectra of high-order above-threshold ionization*

Wu Yan (吴 艳)[a], Ye Hui-Liang (叶会亮)[a],
Zhang Jing-Tao(张敬涛)[a]†, and Guo Dong-Sheng (郭东升)[b]

[a] *State Key Laboratory of High Field Laser Physics, Shanghai Institute of Optics and Fine Mechanics, Chinese Academy of Sciences, Shanghai* 201800, *China*
[b] *Southern University and A&M College, LA* 70813, *USA*

(Received 27 October 2011; revised manuscript received 9 December 2011)

By developing a full quantum scattering theory of high-order above-threshold ionization, we study the energy spectra and the angular distributions of photoelectrons from atoms with intense laser fields shining on them. We find that real rescattering can occur many times, and even infinite times. The photoelectrons from the rescattering process form a broad plateau in the kinetic-energy spectrum. We further disclose a multiple-plateau structure formed by the high-energy photoelectrons, which absorb many photons during the rescattering process. Moreover, we find that both the angular distributions and the kinetic-energy spectra of photoelectrons obey the same scaling law as that for directly emitted photoelectrons.

Keywords: photoelectron energy spectrum, rescattering process, photoelectron angular distribution

PACS: 32.80.Rm, 42.65.Ky, 12.20.Ds, 03.65.Nk **DOI:** 10.1088/1674-1056/21/5/053201

1. Introduction

Photoelectron energy spectra (PES) of high-order above-threshold ionization (ATI) are characterized by a broad plateau ranging from $2U_{\rm p}$ to $10U_{\rm p}$, where $U_{\rm p}$ is the ponderomotive energy. Those high-energy photoelectrons have attracted much attention, both experimentally and theoretically.[1−4] Generally, the generation of those high-energy electrons is described by a so-called "rescattering" mechanism.[5,6] When irradiated by an intense laser field, the bound electrons of atoms or molecules are excited into continuum states which are known as the Volkov states by neglecting the electron–ion interaction. Intuitively, when the electric field of the incident laser reverses, some of the otherwise free electrons in the Volkov states may be pulled back to the vicinity of their parent ions. Most of the driven-back electrons are rescattered, then escape from the laser field rather than combine with the ionic core. The rescattered electrons obtain much higher kinetic energy than those directly ejected, since they are further accelerated by the electric field. Thus, they form the high-energy part of the photoelectron spectrum.

Many theoretical efforts have been devoted to the study of the rescattering process, with both numerical methods[6−8] and analytical approaches,[9−11] in most of which the electric field is treated classically. Although the (quasi-)classical picture explains many phenomena in the strong-field physics, there are still many quantum-field effects. For example, the intense laser field itself can be regarded as a macroscopic quantum state of photons. The fact that the ATI spectrum exhibits discrete peaks isolated by one-photon energy is a substantial demonstration of the quantum feature of intense laser fields. Furthermore, the quantum-field treatment leads to a closed interaction system of photons and matters, in which the energy of the physical system is well defined. A time-independent analytical formula of the ionization rate is obtained, by which one can perform detailed analysis on the studied process. The nonperturbative quantum electrodynamic theory of ATI developed by Guo, Aberg and Creasmann (GAC) is such a treatment,[12]

*Project supported by the National Natural Science Foundation of China (Grant Nos. 10774513, 61078080, 11174304, and 11104167) and the National Basic Research Program of China (Grant Nos. 2010CB923203 and 2011CB808103).

†Corresponding author. E-mail: jtzhang@siom.ac.cn

© 2012 Chinese Physical Society and IOP Publishing Ltd

in which the photon–electron interaction is treated nonperturbatively and quantum mechanically. The theory has interpreted various experimental results, even though the previous calculations were all performed without the rescattering process.[13−17]

In this paper, we derive a full-quantum treatment of high-order ATI based on GAC theory, in which the rescattering is treated as the perturbation of a direct ionization process due to the atomic binding potential. Employing the derived formula, we calculate the PES and the photoelectron angular distributions (PADs) of atoms in strong laser fields. We reveal how significant the rescattering process is to photoelectron spectra. Our calculations show that the PES exhibits a broad plateau followed by a sharp cutoff. We verify that such a plateau is contributed mainly by the rescattering process. We further disclose a multiple-plateau structure formed by the high-energy photoelectrons, which further absorb many photons during the rescattering process. The multiple-plateau structure is visible in many papers both experimentally and theoretically.[18−20] However, it has not attracted enough attention. Moreover, we find that the PADs of rescattered photoelectrons are very sensitive to the attraction of the parent ion, which makes it possible to extract information about the core. Finally, we show that both the PADs and the PES of overall photoelectrons obey the same scaling law as that for the directly emitted photoelectrons. The scaling law provides an effective means to extract information about the target core.

The rest of this article is arranged as follows: in Section 2, we present briefly the Coulomb-corrected transition matrix elements and the corresponding ionization rate formula. In Section 3, we present the numerical results of the PES and the PADs, and verify the scaling law. Section 4 is our conclusions.

2. Transition matrix and ionization-rate formulae

The Hamiltonian of the whole system about a free electron interacting with a laser field of frequency ω reads ($\hbar = c = 1$)

$$H = K + U + V, \tag{1}$$

where[12,21]

$$K = \frac{(-\mathrm{i}\nabla)^2}{2m_\mathrm{e}} + N_\mathrm{a}\omega$$

is the free-electron and free-photon energy operator, and N_a is the photon number operator of the laser field; U denotes the attraction of the parent core to the electron; V is the interaction operator between the electron and the laser, in velocity gauge which reads

$$V = -\frac{e}{m_\mathrm{e}}\boldsymbol{A}(\boldsymbol{r})\cdot(-\mathrm{i}\nabla) + \frac{e^2\boldsymbol{A}^2(\boldsymbol{r})}{2m_\mathrm{e}},$$

where $\boldsymbol{A}(\boldsymbol{r})$ is the vector potential of the quantized laser field.

The non-relativistic quantum-field Volkov states developed by Guo *et al.* are the eigenfunctions of the total Hamiltonian of the system, which are given as[22]

$$|\Psi_{\boldsymbol{P},n}\rangle = V_\mathrm{e}^{-1/2}\sum_{j\geqslant -n}\exp\{\mathrm{i}[\boldsymbol{P}+(u_\mathrm{p}-j)\boldsymbol{k}]\cdot\boldsymbol{r}\} \times \mathcal{X}_{-j}(\zeta,\eta)|n+j\rangle, \tag{2}$$

with the corresponding energy eigenvalues

$$\mathcal{E}_{\boldsymbol{P},n} = \frac{\boldsymbol{P}^2}{2m_\mathrm{e}} + u_\mathrm{p}\omega + (n+1/2)\omega,$$

where $\boldsymbol{P}$ is the momentum of the electron in the laser field, V_e is the normalization volume of the electron; $|n+j\rangle$ are the Fock states of the laser mode with n background photons and j transferred photons; and $u_\mathrm{p}\omega$ is the ponderomotive energy. The (generalized) phased Bessel functions are defined as[23]

$$X_n(z) \equiv J_n(|z|)\,\mathrm{e}^{\mathrm{i}n\varphi}, \quad (\varphi = \arg(z)),$$
$$\mathcal{X}_j(\zeta,\eta) \equiv \sum_{m=-\infty}^{\infty} X_{j-2m}(\zeta)X_m(\eta),$$

where

$$\zeta = 2\sqrt{u_\mathrm{p}/(m_\mathrm{e}\omega)}\boldsymbol{P}\cdot\boldsymbol{\epsilon}, \quad \eta = u_\mathrm{p}\boldsymbol{\epsilon}\cdot\boldsymbol{\epsilon}/2,$$

are complex variables; $\boldsymbol{\epsilon}$ is the polarization vector of the laser mode defined by $\boldsymbol{\epsilon} = \epsilon_x\cos(\xi/2) + \mathrm{i}\epsilon_y\sin(\xi/2)$, where $\xi = 0$ corresponds to linear polarization and $\xi = \pi/2$ to circular polarization. The Volkov states form an orthonormal and complete wavefunction set.

Initially (i.e. $t \to -\infty$), the electron is bounded in the ground state $|\Phi_\mathrm{i}\rangle$, and the background laser photon is n_i. At the scattering moment $t \to 0$, the scattering state is $|\Psi_\mathrm{f}^-\rangle$. According to the formal scattering theory,[24,25] the transition matrix element can be expressed as[12]

$$T_\mathrm{fi} = \langle\Psi_\mathrm{f}^- \mid V \mid \Phi_\mathrm{i}, n_\mathrm{i}\rangle + \langle\Psi_\mathrm{f}^- \mid UG^+V \mid \Phi_\mathrm{i}, n_\mathrm{i}\rangle, \tag{3}$$

where

$$G^+ = \frac{1}{H - K - V - U + \mathrm{i}\epsilon} \tag{4}$$

is the retarded Green's propagator[25,26] marked by the superscript (+), which is used to describe forward propagation. The superscript (−) over $\Psi_{\rm f}$ means the fact that we are dealing with a wave propagating into the past, not future. So the scattering state $|\Psi_{\rm f}^-\rangle$ can be described by the evolution backwards in time as[26]

$$|\Psi_{\rm f}^-\rangle = (1 + G_{\rm V}^- V)\,|\phi_{\rm f}, n_{\rm f}\rangle\,,$$

where $\phi_{\rm f}$ denotes the plan wave state of the free electron, and $n_{\rm f}$ is the final background laser photons, $|\phi_{\rm f}, n_{\rm f}\rangle$ is the final scattering state when $t \to \infty$; and $G_{\rm V}^-$ is an advanced Green's propagator marked by the superscript (−) and used to describe the backward propagation. Within the strong-field approximation, the effect of parent core on the otherwise free electron can be neglected. Thus, according to the scattering theory,[24,25] the Green operators $G_{\rm V}^{\pm}$ can be defined as

$$G_{\rm V}^{\pm} = \frac{1}{H - K - V \pm {\rm i}\epsilon}. \tag{5}$$

Using the Volkov states as the intermediate states, noticing that $V = H - K - U$ and ϵ is infinitesimal, and acting the Green operator $G_{\rm V}^-$ on Volkov states, we find[12]

$$|\Psi_{\rm f}^-\rangle = \sum_{\mathcal{E}_{\boldsymbol{P},n}=\mathcal{E}} |\Psi_{\boldsymbol{P},n}\rangle\,\langle\Psi_{\boldsymbol{P},n}|\phi_{\rm f}, n_{\rm f}\rangle\,. \tag{6}$$

Then, the first term in Eq. (3) can be expressed as

$$T_{\rm fi}^1 = \sum_{\mathcal{E}_{\boldsymbol{P},n}=\mathcal{E}_{\rm f}} \langle\phi_{\rm f}, n_{\rm f} \mid \Psi_{\boldsymbol{P},n}\rangle\langle\Psi_{\boldsymbol{P},n} \mid V \mid \Phi_{\rm i}, n_{\rm i}\rangle, \tag{7}$$

which describes the transition of the electron from the initial bound state to a Volkov state only under the interaction of the laser field, followed by the transition from the Volkov state to the final free state, corresponding to the direct ionization process. The explicit expression of Eq. (7) is given by

$$\begin{aligned} T_{\rm fi}^1 \;=\; & \frac{(u_{\rm p} - j_{\rm i})\omega}{V_{\rm e}^{1/2}} \mathcal{X}_{-j_{\rm i}}(Z_{\rm f}, \eta)^* \\ & \times \mathcal{X}_{-j_{\rm f}}(Z_{\rm f}, \eta)\Phi_{\rm i}(|\boldsymbol{P}_{\rm f} - q\boldsymbol{k}|), \end{aligned} \tag{8}$$

where $j_{\rm i}$, $j_{\rm f}$ are defined in the caption of Fig. 1(a), and the absorbed net number of photons q denotes the order of ATI. In our calculations, we choose $u_{\rm p} = j_{\rm f}$.[12]

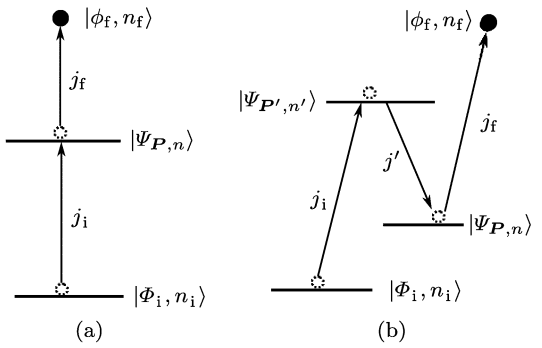


Fig. 1. Schematic illustration of the direct ionization and the rescattering processes. Here, $n_{\rm i}$, n and $n_{\rm f}$ are the background laser photons in initial, Volkov and final states, respectively; $j_{\rm f} = n_{\rm f} - n$ is the number of the emitted laser photons in escaping from the laser field. (a) The direct ionization process. The number of the net absorbed laser photons in direct ionization process is $q = j_{\rm i} - j_{\rm f} = n_{\rm i} - n_{\rm f}$, where $j_{\rm i} = n_{\rm i} - n$, $j_{\rm f} = n_{\rm f} - n$; (b) the rescattering process. The number of the net absorbed laser photons in the rescattering process is $q = j_{\rm i} - j_{\rm f} - j' = n_{\rm i} - n_{\rm f}$, where $j_{\rm i} = n_{\rm i} - n'$, $j' = n - n'$ is the transferred laser photons in the translation of electron between a Volkov state $\Psi_{\boldsymbol{P}',n'}$ and another Volkov state $\Psi_{\boldsymbol{P},n}$.

The second term picking up the binding potential effect of the ionic core on the electron in the laser field is

$$T_{\rm fi}^2 = \sum_{\mathcal{E}_{\boldsymbol{P},n}=\mathcal{E}_{\rm f}} \langle\phi_{\rm f}, n_{\rm f} \mid \Psi_{\boldsymbol{P},n}\rangle\langle\Psi_{\boldsymbol{P},n} \mid UG^+V \mid \Phi_{\rm i}, n_{\rm i}\rangle. \tag{9}$$

Using the identity $G^+ = G_{\rm V}^+ + G_{\rm V}^+ U G^+$, we find

$$UG^+V = UG_{\rm V}^+V + UG_{\rm V}^+UG_{\rm V}^+V + \ldots, \tag{10}$$

with which the second term can be written as

$$\begin{aligned} T_{\rm fi}^2 \;=\; & \sum_{\mathcal{E}_{\boldsymbol{P},n}=\mathcal{E}_{\rm f}} \langle\phi_{\rm f}, n_{\rm f} \mid \Psi_{\boldsymbol{P},n}\rangle\langle\Psi_{\boldsymbol{P},n} \mid UG_{\rm V}^+V \mid \Phi_{\rm i}, n_{\rm i}\rangle \\ & + \sum_{\mathcal{E}_{\boldsymbol{P},n}=\mathcal{E}_{\rm f}} \langle\phi_{\rm f}, n_{\rm f} \mid \Psi_{\boldsymbol{P},n}\rangle \\ & \times \langle\Psi_{\boldsymbol{P},n} \mid UG_{\rm V}^+UG_{\rm V}^+V \mid \Phi_{\rm i}, n_{\rm i}\rangle \\ & + \ldots \end{aligned} \tag{11}$$

Using the following expansion:

$$\begin{aligned} & G_{\rm V}^+V\,|\Phi_{\rm i}, n_{\rm i}\rangle \\ = \; & \frac{1}{H - K - V + {\rm i}\epsilon} V\,|\Phi_{\rm i}, n_{\rm i}\rangle \\ = \; & \sum_{\boldsymbol{P}',n'} \frac{|\Psi_{\boldsymbol{P}',n'}\rangle\,\langle\Psi_{\boldsymbol{P}',n'}|\,V\,|\Phi_{\rm i}, n_{\rm i}\rangle}{H - \mathcal{E}_{\boldsymbol{P}',n'} + {\rm i}\epsilon}, \end{aligned} \tag{12}$$

the first term of Eq. (11) can be expanded as

$$T_{\rm fi}^{21} \;=\; \sum_{\mathcal{E}_{\boldsymbol{P},n}=\mathcal{E}_{\rm f}} \sum_{\boldsymbol{P}',n'} \langle\phi_{\rm f}, n_{\rm f}|\Psi_{\boldsymbol{P},n}\rangle\, \frac{\left\langle\Psi_{\boldsymbol{P},n}\,|U|\,\Psi_{\boldsymbol{P}',n'}\right\rangle}{\mathcal{E}_{\boldsymbol{P},n} - \mathcal{E}_{\boldsymbol{P}',n'} + {\rm i}\epsilon}$$

$$\times \left\langle \Psi_{\boldsymbol{P}',n'} \left| V \right| \Phi_{\rm i}, n_{\rm i} \right\rangle, \quad (13)$$

where the first factor, from the right, describes the excitation of an initially bound electron to a virtual, or real, Volkov state under the action of the laser field; the third factor describes the exit process of the electron from the Volkov state to a free photoelectron detected experimentally; the second factor describes the transition from a Volkov state to another Volkov state under the attraction of the parent core. Thus, the $T_{\rm fi}^{21}$ term describes the generation process of photoelectrons once rescattered by the ionic core. As shown in Eq. (11), the rescattering under the action of the ionic core can occur once, twice, ..., n times, ... The number of rescattering times is unbounded. The first time rescattering process is depicted explicitly in Fig. 1(b).

The derivations of the first and the last factors in Eq. (13) are straightforward, and the middle factor is worked out to be

$$\begin{aligned} &\langle \Psi_{\boldsymbol{P},n} \mid U \mid \Psi_{\boldsymbol{P}',n'} \rangle \\ &= V_{\rm e}^{-1} U(\boldsymbol{P} - \boldsymbol{P}' + (n-n')\boldsymbol{k}) X_{n'-n}(\zeta' - \zeta), \end{aligned} \quad (14)$$

where $U(\boldsymbol{P})$ is the Fourier transform of the binding potential of the ionic core. For the screened Coulomb potential

$$U(r) = -\frac{Ze^2}{4\pi r} \exp(-\lambda r),$$

where Z is the number of the nuclear charge and λ is the screening parameter, it is given by

$$U(\boldsymbol{P} - \boldsymbol{P}') = \frac{-Ze^2}{|\boldsymbol{P} - \boldsymbol{P}'|^2 + \lambda^2}. \quad (15)$$

In deriving Eq. (14), we have used the subtraction theorem of generalized phased Bessel (GPB)functions[23]

$$\sum_{q=-\infty}^{\infty} \mathcal{X}_{n+q}(z_{\rm c_1}, z_{\rm s}) \mathcal{X}_q(z_{\rm c_2}, z_{\rm s})^* = X_n(z_{\rm c_1} - z_{\rm c_2}). \quad (16)$$

Using the formula

$$|\Phi_{\rm i}(\boldsymbol{P})|_{\rm av}^2 = 4\pi |\Phi_{n_{\rm i} l_{\rm i}}(|\boldsymbol{P}|)|^2,$$

where the subscript av means averaging over the magnetic quantum numbers and

$$\Phi_{n_{\rm i} l_{\rm i}}(|\boldsymbol{P}|) = \int_0^\infty r \,{\rm d}r P_{n_{\rm i} l_{\rm i}}(r) j_{l_{\rm i}}(|\boldsymbol{P}|r),$$

we can reduce the initial momentum wavefunction as

$$\begin{aligned} &|\Phi_{\rm i}(\boldsymbol{P}' + (u_{\rm p} - j')\boldsymbol{k})|_{\rm av} \\ &= \sqrt{4\pi} \left| \Phi_{\rm i}(|\boldsymbol{P}' + (u_{\rm p} - j')\boldsymbol{k}|) \right|. \end{aligned} \quad (17)$$

Finally, we express the transition matrix element as

$$\begin{aligned} T_{\rm fi}^{21} = &-\frac{Ze^2\omega}{4V_{\rm e}^{1/2}\pi^{5/2}} \\ &\times \sum_{j_{\rm i}} \int {\rm d}\boldsymbol{P}' \left\{ \frac{X_{q-j_{\rm i}+j_{\rm f}}(\zeta' - \zeta_{\rm f}) \mathcal{X}_{-j_{\rm f}}(\zeta_{\rm f}, \eta)}{|\boldsymbol{P}_{\rm f} - \boldsymbol{P}' - q\boldsymbol{k}|^2 + \lambda^2} \right. \\ &\left. \times \mathcal{X}_{-j_{\rm i}}(\zeta', \eta)^* (u_{\rm p} - j_{\rm i}) \Phi_{\rm i}(|\boldsymbol{P}'|) \frac{1}{\Delta\mathcal{E} + {\rm i}\epsilon} \right\}, \end{aligned} \quad (18)$$

where $j_{\rm i}$, $j_{\rm f}$ are defined in the caption of Fig. 1 (b); and $\Delta\mathcal{E} = \mathcal{E}_{\boldsymbol{P},n} - \mathcal{E}_{\boldsymbol{P}',n'}$ is the energy difference between the two involved Volkov states. With the relations

$$\frac{1}{\Delta\mathcal{E} + {\rm i}\epsilon} = -\frac{{\rm i}\epsilon}{\Delta\mathcal{E}^2 + \epsilon^2} + \frac{\Delta\mathcal{E}}{\Delta\mathcal{E}^2 + \epsilon^2},$$

$$\lim_{\epsilon \to 0} \frac{\epsilon}{\left(\mathcal{E}_{\boldsymbol{P},n} - \mathcal{E}_{\boldsymbol{P}',n'}\right)^2 + \epsilon^2} = \pi \delta(\mathcal{E}_{\boldsymbol{P}n} - \mathcal{E}_{\boldsymbol{P}'n'}), \quad (19)$$

and noticing $\mathcal{E}_{\boldsymbol{P},}n = \mathcal{E}_{\rm f}$, we express the delta function as

$$\begin{aligned} &\delta(\mathcal{E}_{\rm f} - \mathcal{E}_{\boldsymbol{P}',n'}) \\ &= \left(\frac{m_{\rm e}}{2\omega}\right)^{1/2} (j_{\rm i} - u_{\rm p} - \varepsilon_{\rm b})^{-1/2} \\ &\quad \times \delta\left[P' - (2m_{\rm e}\omega)^{1/2} (j_{\rm i} - u_{\rm p} - \varepsilon_{\rm b})^{1/2}\right], \end{aligned}$$

where $\varepsilon_{\rm b}$ is the binding number, i.e., the binding energy per laser photon energy. The delta function in Eq. (19) guarantees the energy conservation, so the related transition is a physically real process. According to the above description, we rewrite Eq. (18) as

$$T_{\rm fi}^{21} = \frac{\omega}{V_{\rm e}^{1/2}} \frac{Ze^2}{4\pi^{5/2}} \left(T_{\rm fi}^{\rm r} + T_{\rm fi}^{\rm n}\right). \quad (20)$$

The first term in Eq. (20) denotes the on-energy-shell transitions in which the involved Volkov states are of the same eigenenergy, and is worked out to be

$$\begin{aligned} &T_{\rm fi}^{\rm r} \\ &= -{\rm i}\pi m_{\rm e} \sum_{j_{\rm i}} \int {\rm d}\Omega_{\boldsymbol{P}'} \{ X_{q-j_{\rm i}+j_{\rm f}}(\zeta' - \zeta_{\rm f}) \\ &\quad \times \frac{\mathcal{X}_{-j_{\rm f}}(\zeta_{\rm f}, \eta) \mathcal{X}_{-j_{\rm i}}(\zeta', \eta)^* (j_{\rm i} - u_{\rm p}) |\boldsymbol{P}'| \Phi_{\rm i}(|\boldsymbol{P}'|)}{|\boldsymbol{P}_{\rm f} - \boldsymbol{P}' - q\boldsymbol{k}|^2 + \lambda^2} \}, \end{aligned} \quad (21)$$

with $|\boldsymbol{P}'| = (2m_{\rm e}\omega)^{1/2}(j_{\rm i} - u_{\rm p} - \varepsilon_{\rm b})^{1/2}$. The second term of Eq. (20) denotes the off-energy-shell transitions in which the involved Volkov states are of unequal eigenenergies, and is given by

$$T_{\rm fi}^{\rm n} = \sum_{j_{\rm i}} \int {\rm d}\boldsymbol{P}'$$

$$\times \left\{ \frac{X_{q-j_{\rm i}+j_{\rm f}}(\zeta'-\zeta_{\rm f})\mathcal{X}_{-j_{\rm f}}(\zeta_{\rm f},\eta)\mathcal{X}_{-j_{\rm i}}(\zeta',\eta)^*}{|\boldsymbol{P}_{\rm f}-\boldsymbol{P}'-q\boldsymbol{k}|^2+\lambda^2} \right.$$
$$\left. \times \frac{(j_{\rm i}-u_{\rm p})\Phi_{\rm i}(|\boldsymbol{P}'|)}{\Delta\mathcal{E}} \right\}, \quad (22)$$

with $\Delta\mathcal{E}=(j_{\rm i}-u_{\rm p}-\varepsilon_{\rm b})\omega-|\boldsymbol{P}'|^2/2m_{\rm e}$.

The real processes conserve both the total energy and the total momentum, in contrast with the virtual transitions which do not conserve energy. Numerical calculation shows that the real rescattering process is much stronger in transition rates than in the virtual rescattering process. The transition between a Volkov state and another Volkov state with conserved energy indicates a real physical process, which does actually occur. With a solid theoretical proof of the existence of the rescattering process, the study of any observable phenomena relating to the real rescattering can be called a rescattering effect.

The total ionization rate can be obtained by the standard treatment in the scattering theory. The differential ionization rate for a given ATI order q reads

$$\frac{{\rm d}W}{{\rm d}\Omega_{\boldsymbol{P}_{\rm f}}} = \frac{V_{\rm e}}{(2\pi)^2}\int |\boldsymbol{P}_{\rm f}|^2\,{\rm d}P_{\rm f}\left|T_{\rm fi}^1+T_{\rm fi}^{21}\right|^2\delta(\mathcal{E}_{\rm i}-\mathcal{E}_{\rm f})$$
$$= \frac{(2m_{\rm e}^3\omega^5)^{1/2}}{(2\pi)^2}(q-\varepsilon_{\rm b})^{1/2}|\tilde{T}_{\rm fi}^1+\tilde{T}_{\rm fi}^{21}|^2, \quad (23)$$

where the tilde placed over the transition matrix element means which is divided by $\omega V_{\rm e}^{-1/2}$, i.e., $\tilde{T}=T/(\omega V_{\rm e}^{-1/2})$.

3. Numerical results and discussion

In this section, using the derived ionization rate formula, we calculate PES and PADs of atoms in various laser fields. Without further statement, the laser field is chosen as that from Ti:S laser system of wavelength 800 nm with intensity varying from 10^{13} to 10^{15} W/cm^2, and the target atom is chosen as the hydrogen atom with ionization potential 13.6 eV. The second transition matrix element in Eq. (23) contains the on-energy-shell transitions and the off-energy-shell transitions. Due to the large denominator in the fraction of Eq. (22), mathematically, the transitions between the Volkov states with unequal energy eigenvalues play a trivial role compared with the on-energy-shell transitions. Moreover, our numerical calculations verify that the contribution of the off-energy-shell transition to ionization rate is, generally, at least three orders of magnitude less than that of on-energy-shell transitions. Thus, our calculations only involve the on-energy-shell transitions.

3.1. Kinetic-energy spectra and angular distributions of high-energy photoelectrons

The calculated PES and PADs are shown in Figs. 2 and 3. Figure 2 depicts the calculated kinetic-energy spectra at laser intensity of 1.56×10^{14} W/cm^2. We see from the figure that the spectrum of overall photoelectrons from both the direct ionization and the rescattering processes shows a fast decrease at the low-order part, then exhibits a plateau in the middle part, and then a sharp decrease appears at ATI orders higher than 70. For comparison, the contribution of $T_{\rm fi}^1$ term is also depicted. The photoelectrons from $T_{\rm fi}^1$ term contribute mainly to the low energy part, and the yield decreases quickly as the ATI order increases. The numerical result discloses that the yield of photoelectrons from $T_{\rm fi}^{21}$ term forms the plateau running up to about the 70th ATI order. For lower ATI orders, the yield from $T_{\rm fi}^{21}$ term is far less than that from $T_{\rm fi}^1$ term, then the low-order ATI electrons are mainly from the direct ionization mechanism. Due to the fast decrease, the yield from $T_{\rm fi}^1$ term becomes less than that from $T_{\rm fi}^{21}$ for ATI orders higher than 40. Thus, the higher-order ATI photoelectrons are mainly from the $T_{\rm fi}^{21}$ transitions. The result coincides with that in Ref. [27] theoretically, and Ref. [6] experimentally. For the chosen laser intensity, the ponderomotive parameter is 6.0, and the minimum photons absorbed to overcome the binding potential is about 9, we see that the plateau cuts off at about $10U_{\rm p}$, while the plateau begins a little higher than the generally accepted $2U_{\rm p}$. The calculated spectrum for circularly polarized laser field shows no plateau, which agrees well with the previous studies.

Detailed study discloses that the Bessel function $X_{q-j_{\rm i}+j_{\rm f}}(\zeta'-\zeta_{\rm f})$ arising from the transition between Volkov states in the transition rate formula plays a key role in forming the plateau. Since $j_{\rm i}$ denotes the number of absorbed photons in the ionization process, it determines the momentum of the electron in a Volkov state, so we define one $j_{\rm i}$ as an excitation channel. Calculations indicate that the plateaus of different channels cut off at different regions, and generally, the channels with small $j_{\rm i}$ cut off at a lower energy region,

but with higher probabilities. For the channels with higher j_i, the cutoffs appear at energy much larger than $10U_p$. However, the interference among different channels eliminates the higher-energy plateaus, so the overall plateau cuts off at about $10U_p$. For circular polarization, each ionization channel exhibits a plateau, but the interference effect shortens the length and decreases the height of the overall plateau, so the plateau formed by rescattered photoelectrons is covered by that formed by the direct-emitted photoelectrons. As a result, the overall spectrum shows no plateau in a circular polarized laser field.

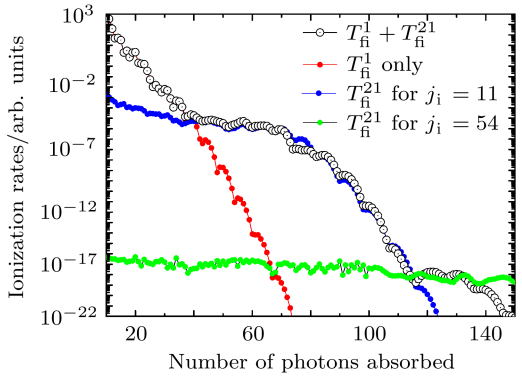


Fig. 2. (colour online) The calculated kinetic energy spectra of photoelectrons in linearly polarized laser field of intensity 1.56×10^{14} W/cm^2 and wavelength 800 nm. The abscissa is the number of net laser photons absorbed during ionization. The value of λ is chosen to be 0.1.

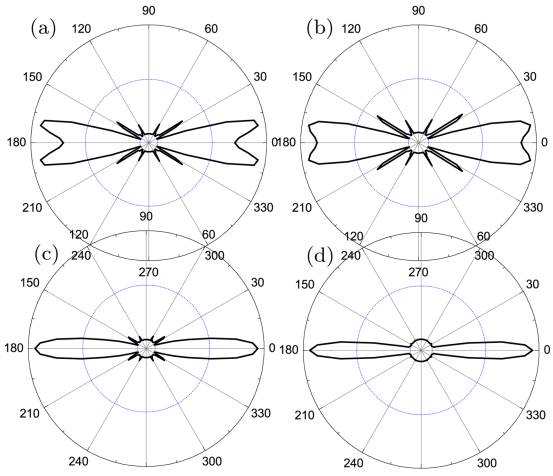


Fig. 3. PADs of the 23rd ATI peak for hydrogen atoms irradiated by a laser field of wavelength 800 nm and intensity 1.04×10^{14} W/cm^2 for different values of λ: (a) 0.01, (b) 0.05, (c) 0.1, and (d) 0.2. For comparison, the PADs are normalized.

Our calculations on different channels disclose that the photoelectrons may exchange photons with the laser field during the rescattering process, emitting photons or further absorbing photons. Take the channel of $j_i = 15$ as an example, the bound electron absorbs 15 photons during its excitation into a continuum state. When it is rescattered by the parent core, it may emit several photons, which contributes to the ATI peaks lower than the 15th order. While more generally, it further absorbs photons contributing to the ATI peaks higher than the 15th order. All the transitions are of comparable probabilities, so the PES from this channel exhibits a long plateau with a cutoff at about the 100th ATI order. The photoelectrons are more likely to further absorb photons in the rescattering process, which confirms the assumption that the photoelectrons are accelerated during the rescattering process. For a given ATI order, many channels contribute to it and the interference effect among channels is important.

Our calculations reveal a multiple-plateau structure in the PES, as shown in Fig. 2 for the total ionization rate. Here, the "multiple-plateau" denotes the plateau structure except the one discussed above and includes two aspects. One is the short plateau cutting off around the 80th ATI order, and the other denotes the long plateau following the 115th ATI order. Mathematically, the GPB function $\mathcal{X}_{-j_f}(\zeta_f, \eta)$ arising from the exit process[13] causes the short plateau, thus the plateau is formed when the photoelectrons leave the laser field. This plateau is evident for a fixed laser intensity and becomes not so notable when the laser intensity fluctuates. In fact, the PES in the cutoff region shows many trivial rises and falls, each may be regarded as such a plateau. The low-order ATI channels contribute to the first plateau and their oscillation forms the short plateau in the PES, as shown in Fig. 2 for $j_i = 11$. The long plateau appears for very high ATI order and is ascribed to the multi-rescattering of photoelectrons in the past.[20,28] Here, we argue that this plateau is formed by high-order ATI channels, as shown in Fig. 2. The ionization rate for $j_i = 54$ channel exhibits a very long plateau with a small value. The contribution of this channel to lower order ATI peaks is quite trivial, but becomes important for ATI peaks in the second plateau. Note that in our calculations only the first time rescattering is included, so we identify that the second plateau is formed by high-order ATI channels.

For directly emitted photoelectrons, the PADs are determined by the GPB function that describes the

physical process, thus determined by the number of photons absorbed during the ionization and the ponderomotive parameter of the laser field in turn. For rescattered photoelectrons, the kinetic energy has no relation with the number of photons absorbed during ionization, say $j_{\rm i}$ in Eq. (21). The number role of jets in PADs does not hold yet, since too many channels contribute to one rescattering ATI peak. Consequently, the PADs are determined by many factors and show complicated structures. The PADs exhibit many huge jets striking away from the waist of the main lobes along the laser polarization, and the main lobes may split distinctively. Moreover, the motion of electrons is affected by the Coulomb attraction of the parent ion during rescattering, while the latter is characterized by the value of λ. Then, the PADs become very sensitive to the value of λ. Figure 3 depicts the PADs of the 23rd ATI peak for different values of λ, from which we see the PADs show the main lobes along the laser polarization. Such kind of PADs agrees with the experimental observation in Ref.[3]. The height of jet varies with the value of screening parameter λ, and the main lobes split as the value of λ decreases. The distinctive variation of PADs with λ inspires people to attract the information of binding potential by the PADs of rescattering photoelectrons, as did by Okunishi *et al.* to retrieval the cross section of the parent ion by the rescattering electrons.[29,30]

3.2. Scaling relation of high-energy photoelectrons

Scaling analysis is a powerful technique for analyzing many phenomena in strong field physics. For example, many papers have contributed to the scaling relation of high-order harmonic generation.[31,32] For photoionization, our analytical study has shown that the main features of angular distributions of directly emitted photoelectrons are mainly determined by three dimensionless parameters: 1) $u_{\rm p}$, the ponderomotive number; 2) $\varepsilon_{\rm b}$, the binding number; 3) the orders of ATI peaks. Keeping the three physical quantities unchanged, the physical process is identical, and a scaling law of PADs is established.[33] The scaling law states that for corresponding ATI peaks, the PADs from an atom with the binding energy $E_{\rm b}$ irradiated by a laser beam of intensity I and frequency ω are the same as those from an atom with the binding energy $kE_{\rm b}$ irradiated by a laser beam with intensity k^3I and frequency $k\omega$. While for rescattered photoelectrons, does the scaling relation still hold?

We first study the scaling relation on the PADs of rescattered photoelectrons. We do as follows: choose the PADs of an ATI peak in the plateau as a reference, change the binding energy and the laser frequency to k times, and change the laser intensity to k^2, k^3 and k^4 times the original, respectively, then compare the main features of the calculated PADs. Figure 4 shows such a comparison. We see the PADs related with the physical quantities chosen as the scaling law are the same, while the other two patterns of PADs show more or less differences from the original one. Thus, we conclude that the PADs of rescattered electrons obey the scaling law.

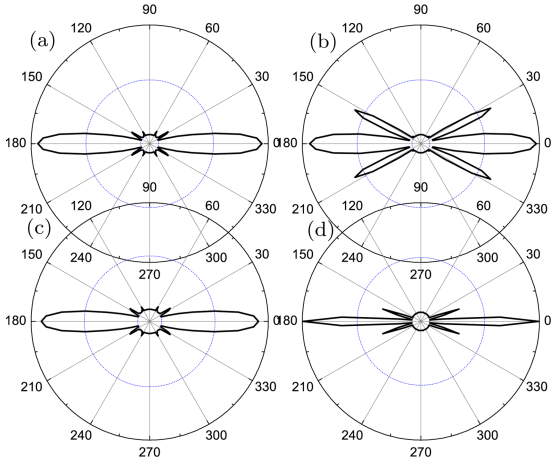


Fig. 4. (a) PADs of the 23rd ATI peak for hydrogen atoms irradiated by a laser field of wavelength 800 nm and intensity 1.04×10^{14} W/cm^2. (b) –(d) PADs of the 23rd ATI peak for a model atom of ionization potential 27.2 eV irradiated by a laser field of wavelength 400 nm and laser intensities (b) 4.16×10^{14}, (c) 8.32×10^{14} and (d) 16.64×10^{14} W/cm^2. The value of λ for (a) is chosen as 0.1, while it is 0.2 for the other three.

The energy spectra of rescattered photoelectrons also obey the scaling law. Noticing that in the unit of photon energy, the plateau cuts off at about an ATI order around $10u_{\rm p}$, while one important feature of the scaling law is to keep $u_{\rm p}$ unchanged. Thus, we wonder whether the scaling law still holds in the energy spectra. By changing the three quantities according to the scaling law, we calculate the spectrum and compare it with the original one. The comparison is shown in Fig. 5. Although the scaled emission rates are little higher than the original, the variations of the spectra are almost the same as each other, both for directly emitted and for rescattered photoelectrons.

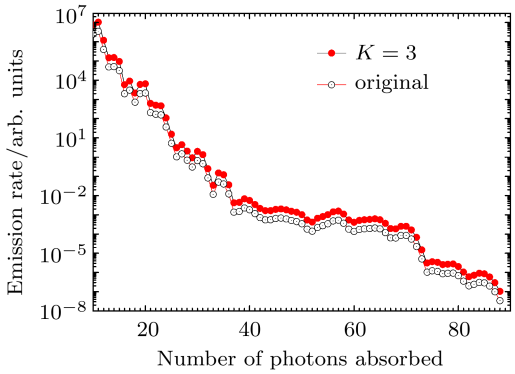


Fig. 5. (colour online) Comparison of kinetic-energy spectra of photoelectrons: black open circles denote the emission rates from hydrogen atoms in a laser field of wavelength 800 nm and intensity 1.56×10^{14} W/cm^2, and red real circles denote those from a model atom with binding energy 40.8 eV in laser field of wavelength 267 nm and intensity 4.21×10^{15} W/cm^2. The abscissas is the number of net photons absorbed by the electrons during ionization. The value of λ is chosen as 0.27.

4. Conclusion

We conclude as follows:

1) Rescattering processes exist in multiple-photon ionization, as real transitions between a real Volkov state and another real Volkov state with both energy and momentum conservation. The rescattering can occur many times, even infinite times. The rescattering processes contribute photoelectron production rates to photoelectron spectra significantly.

2) For a linearly polarized laser field, the kinetic-energy spectrum of photoelectrons exhibits a broad plateau followed by a sharp cutoff at about $10U_{\rm p}$. The plateau is formed by the rescattered photoelectrons. For circular polarization, the PES does not exhibit any plateau structure.

3) We show a multiple-plateau structure of PES in laser fields with linear polarization. Besides the plateau cutting off at $10U_{\rm p}$, there is a second plateau appears around between $17U_{\rm p}$ and $23U_{\rm p}$, which is formed by the high-order ATI channels, i.e., when the bound electrons absorb many photons in the excitation process and further absorb photons during the rescattering process.

4) The angular distributions and the kinetic-energy spectra of rescattered photoelectrons obey the same scaling law as those of the directly emitted photoelectrons, which indicates that the binding parameter, the ponderomotive parameter, and the ATI order are the three basic parameters in the photoionization process.

References

[1] Choi N N, Jiang T F, Morishita T, Lee M H and Lin C D 2010 *Phys. Rev.* A **82** 013409

[2] Lin C D, Le A T, Chen Z, Morishita T and Lucchese R 2010 *J. Phys.* B: *At. Mol. Opt. Phys.* **43** 122001

[3] Cornaggia C 2009 *J. Phys.* B: *At. Mol. Opt. Phys.* **42** 161002.

[4] Xu J, Chen Z, Le A T and Lin C D 2010 *Phys. Rev.* A **82** 033403

[5] Krausz F and Ivanov M 2009 *Rev. Mod. Phys.* **81** 163

[6] Yang B, Schafer K J, Walker B, Kulander K C, Agostini P and DiMauro L F 1993 *Phys. Rev. Lett.* **71** 3770

[7] Morishita T, Le A T, Chen Z and Lin C D 2008 *Phys. Rev. Lett.* **100** 013903

[8] Wickenhauser M, Tong X M, Arbo D G, Burgdorfer J and Lin C D 2006 *Phys. Rev.* A **74** 041402(R)

[9] Paulus G G, Becker W, Nicklich W and Walther H 1994 *J. Phys.* B: *At. Mol. Opt. Phys.* **27** L703

[10] Lewenstein M, Kulander K C, Schafer K J and Bucksbaum P H 1995 *Phys. Rev.* A **51** 1495

[11] Xin G, Ye D, Zhao Q and Liu J 2011 *Acta Phys. Sin.* **60** 093204

[12] Guo D S, Åberg T and Crasemann B 1989 *Phys. Rev.* A **40** 4997

[13] Zhang J, Zhang W, Xu Z, Li X, Fu P, Guo D S and Freeman R R 2002 *J. Phys.* B: *At. Mol. Opt. Phys.* **35** 4809

[14] Bai L, Zhang J, Xu Z and Guo D S 2006 *Phys. Rev. Lett.* **97** 193002

[15] Zhang J, Woerkom L D, Guo D S and Freeman R R 2007 *Phys. Rev.* A **76** 015401

[16] Bucksbaum P H, Schumacher D W andBashkansky M 1988 *Phys. Rev. Lett.* **61** 1182

[17] Guo D S and Drake G W F 1992 *Phys. Rev.* A **45** 6622

[18] Nandor M J, Walker M A and VanWoerkom L D 1998 *J. Phys.* B: *At. Mol. Opt. Phys.* **31** 4617

[19] Milošević D B and Ehlotzky F 1999 *J. Phys.* B: *At. Mol. Opt. Phys.* **32** 1585

[20] Usachenko V I and Pazdzersky V A 2004 *Phys. Rev.* A **69** 013406

[21] Wang B B, Gao L, Li X, Guo D S and Fu P 2007 *Phys. Rev.* A **75** 063419

[22] Guo D S and Drake G W F 1992 *J. Phys.* A: *Math. Gen.* **25** 3383

[23] Wang Y, Zhang J T, Ren X H and Xu Z Z 2009 *Chin. Phys.* B **18** 4815

[24] Lippmann B and Schwinger J 1950 *Phys. Rev.* **79** 469

[25] Gell-Mann M and Golberger M L 1953 *Phys. Rev.* **91** 398

[26] Greiner W · Reinhardt J 2003 *Quantum Electrodynamics* 3rd ed (Germany: Spinger) pp.1–20

[27] Chen Z J, Le A T, Morishita T and Lin C D 2009 *J. Phys.* B: *At. Mol. Opt. Phys.* **42** 061001

[28] Hertlein M P, Bucksbaum P H and Muller H G 1997 *J. Phys.* B: *At. Mol. Opt. Phys.* **30** L197

[29] Okunishi M, Morishita T, Prumper G, Shimada K, Lin C D, Watanabe S and Ueda K 2008 *Phys. Rev. Lett.* **100** 143001

[30] Morishita T, Okunishi M, Shimada K, Pruper G, Chen Z, Watanabe S, Ueda K and Lin C D 2009 *J. Phys.* B: *At. Mol. Opt. Phys.* **42** 105205

[31] Tate J, Auguste T, Muller H G, Salieres P, Agostini P and DiMauro L F 2007 *Phys. Rev. Lett.* **98** 013901

[32] Pérez-Hernández J A, Ramos J, Roso L and Plaja L 2010 *Laser Phys.* **20** 1044

[33] Guo D S, Zhang J, Xu Z, Li X, Fu P and Freeman R R 2003 *Phys. Rev.* A **68** 043404